Influence of dopants and substrate material on the formation of Ga vacancies in epitaxial GaN layers

J. Oila, V. Ranki, J. Kivioja, K. Saarinen, and P. Hautojärvi
Laboratory of Physics, Helsinki University of Technology, P.O.Box 1100, FIN-02015 HUT, Espoo, Finland

J. Likonen
Technical Research Centre of Finland, Chemical Technology, P.O. Box 1404, FIN-02044 VTT, Espoo, Finland

J. M. Baranowski and K. Pakula
Institute of Experimental Physics, University of Warsaw, 00-681 Warsaw, Poland

T. Suski, M. Leszczynski, and I. Grzegory
UNIPRESS, High Pressure Research Center, Polish Academy of Sciences, 01-142, Warsaw, Poland

We have applied a low-energy positron beam and secondary ion mass spectrometry to study defects in homoepitaxial and heteroepitaxial GaN layers. Positron experiments reveal high concentrations of Ga vacancies in nominally undoped n-type GaN, where the conductivity is due to unintentional oxygen incorporation. Ga vacancies are observed in both homoepitaxial and heteroepitaxial layers, indicating that their formation is independent of the dislocation density. No Ga vacancies are detected in p-type or semi-insulating samples doped with Mg, as predicted by the theoretical formation energies. In samples where n-type conductivity is due to Si doping and the incorporation of oxygen impurities is suppressed, the concentration of Ga vacancies is much lower than in n-type samples containing oxygen. This indicates that the presence of oxygen donor in GaN promotes the formation of Ga vacancy. We suggest that this effect is due to the creation of V_{Ga}-O_N complexes during the epitaxial growth.

I. INTRODUCTION

The considerable progress in GaN-based semiconductor technology during the recent years has already led to the commercial launching of short wavelength light emitting diodes and laser diodes. This manufacturing success has been achieved despite the fact that many of the materials properties and characteristics are not fully understood. The epitaxial GaN layers, most often grown by metal organic chemical vapor deposition (MOCVD) on a sapphire substrate, typically contain high densities of both extended and point defects which have a significant influence on the electrical and optical properties of the layer. For high performance applications the detailed knowledge on the formation and the nature of these defects is needed.

The lattice-mismatch between the GaN layer and the sapphire substrate may lead to dislocation densities as high as 10^{10} cm^{-2}. The role of dislocations and other extended defects in the physical properties of GaN has been widely studied,[1-6] but much less is known about the role of point defects. Among native point defects in GaN, the formation energy of antisites and interstitials has been calculated and found to be too high for them to exist in significant concentrations.[7] The formation energies of the vacancies are calculated to be lower: the dominating native defect in p-type GaN is expected to be the N vacancy and in n-type GaN the Ga vacancy.[7] The N vacancy is reported to act as a shallow donor,[8] and it is suggested that it behaves as a potential compensating defect in Mg-doped GaN grown at high temperatures.[9] The N vacancy has also been suggested to

cause the n-type conductivity observed in undoped GaN,[10,11] but in later studies the n-type conductivity was associated to residual O or Si impurities.[7,12,13] The gallium vacancy V_{Ga} acts as a deep acceptor[14] and is suggested to be responsible for the carrier compensation in n-type GaN.[15,16] The formation of complexes between the Ga vacancy and donor-impurities O or Si is calculated[14,17] to be energetically favored and the energy levels of the complexes are suggested to be involved in the emission of the parasitic yellow luminescence.[14,17,18]

Positron annihilation is an effective tool for studying vacancy-type defects in semiconductors.[19-21] Positrons get trapped at vacancies due to the missing positive ion core at vacancy site.[22] The trapping is experimentally observed in two ways: as a narrowing of the momentum distribution of the annihilating electron–positron pair and as an increase in the positron lifetime. The annihilation data can be used to estimate the vacancy concentration with a sensitivity in the range of 10^{16}–10^{19} cm^{-3}. The annihilation data gives information on the nature of the atoms around the vacancy and enables distinguishing between vacancies in different sublattices. Previous positron studies on GaN have shown that gallium vacancies are present both in undoped n-type GaN epitaxial layers and bulk crystals.[23,24] The concentration of vacancies has been found to correlate with the intensity of the yellow luminescence[24] and with the V/III molar ratio used during growth.[16]

In our present positron annihilation study the aim is to clarify the influence of doping on the formation of point defects in both homoepitaxial and heteroepitaxial GaN lay-

TABLE I. The charge carrier concentrations and mobilities in studied GaN layers. The Ga vacancy concentrations are estimated from positron annilation experiments.

Doping	Substrate	Carrier concentration (cm^{-3})	μ ($cm^2\,V^{-1}\,s^{-1}$)	Ga vacancy concentration (cm^{-3})
1. Mg (annealed at 750 °C)	Al_2O_3	$p \sim 2 \times 10^{17}$	14	$\leqslant 10^{16}$
2. Mg	Al_2O_3	semi-insulating		$\leqslant 10^{16}$
3. undoped (O)	Al_2O_3	$n = 3.7 \times 10^{17}$	190	2×10^{18}
4. undoped (O)	Al_2O_3	$n = 7.0 \times 10^{17}$	150	2×10^{17}
5. undoped (O)	GaN	n		8×10^{17}
6. Si	Al_2O_3	$n = 1.3 \times 10^{17}$	730	$\leqslant 10^{16}$
7. Si	Al_2O_3	$n = 5.3 \times 10^{17}$	516	$\leqslant 10^{16}$
8. Si	Al_2O_3	$n = 1.38 \times 10^{18}$	354	$\leqslant 10^{16}$
9. Si	Al_2O_3	$n = 5.1 \times 10^{18}$	204	$\leqslant 10^{16}$

ers. We detect Ga vacancies in nominally undoped n-type material but not in Mg-doped semi-insulating or p-type layers. The Ga vacancies are observed also in n-type homoepitaxial GaN, thus demonstrating that their formation does not require the presence of dislocations. The Ga vacancy concentration is, however, smaller in n-type layers doped with silicon than in those doped with oxygen. This result leads us to associate the observed Ga vacancy to a V_{Ga}–O_N complex and to suggest that in the presence of oxygen the formation of Ga vacancies is enhanced via the formation of V_{Ga}–O_N complexes.

II. EXPERIMENTAL

A. Samples

We studied Mg-doped p-type, semi-insulating (SI), nominally undoped, and Si-doped n-type GaN epilayer samples. All studied layers had been grown at the Institute of Experimental Physics, University of Warsaw. The charge carrier concentrations and carrier mobilities in the studied samples are given in Table I. In all epitaxial samples the GaN layer was grown on a Al_2O_3 substrate in atmospheric-pressure MOCVD equipment with the gas system and the quartz reactor specially designed for the growth of nitride compounds. Ammonia and trimethylgallium were used as source gases, and hydrogen was used as a carrier gas. The p-type conductivity was achieved by Mg-doping, followed by thermal annealing at 750° C for 15 min. In the semi-insulating (SI) sample the residual n-type conductivity was compensated by heavy Mg-doping without thermal annealing. As a reference sample, we studied a heavily Mg-doped GaN single crystal, on which positron lifetime experiments have been previously performed.[25] The GaN single crystal had been grown in High Pressure Research Center, Polish Academy of Sciences. The studied nominally undoped GaN layers show strong n-type conductivity with $n = 10^{17}$–10^{18} cm^{-3}. This is most probably caused by residual oxygen impurities. In fact, the secondary ion mass spectrometry (SIMS) experiments showed that the concentration of oxygen in epitaxial layers was $> 10^{18}$ cm^{-3}, which is enough to explain the n-type conductivity.

The effect of silicon doping on the formation of Ga vacancies was investigated by studying a set of 3–4 μm thick GaN:Si layers. The concentration of Si dopants was shown to be clearly higher than the concentration of residual oxygen impurities as determined by both magneto-optical measurements[26] and SIMS experiments. The free electron density n, determined by Hall measurements, varied in range 5×10^{17}–5×10^{18} cm^{-3}. The GaN epilayers grown on sapphire substrate typically contain a very high density, $\sim 10^{10}$ cm^{-2}, of dislocations. To study the effect of the layer structural quality on the formation of Ga vacancies, a nominally undoped n-type GaN layer grown on a Mg-doped bulk GaN crystal was also investigated.

B. Positron annihilation spectroscopy

Positron annihilation experiments were performed using a low-energy positron beam. After implantation into a solid, positrons thermalize in few picoseconds. Thermalized positrons diffuse in the lattice until they annihilate with electrons. Vacancies in neutral or negative charge states act as efficient traps for positrons. At a vacancy the average electron density is lower, leading to an increase in the lifetime of trapped positrons. In addition, trapping at vacancies leads to the narrowing of the momentum distribution of annihilating e^+e^- pairs, which is measured by the Doppler broadening of the 511 keV annihilation line. Positrons are also sensitive to negative ion-type acceptors. Positrons get trapped at Rydberg states around negative ions, but due to low binding energy the trapping is effective only at low temperatures, typically at $T < 200$ K.[20] Since the surroundings of negative ions do not contain open volume, the positron lifetime and the momentum distribution in this state are similar to those in the perfect lattice. The positron spectroscopy thus enables the direct observation of neutral and negative open-volume defects and distinguishes efficiently between vacancies and negative ions. Positrons are not, however, trapped at positive centers before they annihilate with electrons.

In conventional positron beam measurements the main observable is the Doppler broadening of the annihilation line. The annihilation spectra are recorded using a Ge detector

with a resolution of 1.3 at 511 keV. The broadening is described by the shape parameters S and W.[20] The low-momentum parameter S is determined as the fraction of counts in the central area of the peak, corresponding to a longitudinal momentum component of $p_L \lesssim 3.7 \times 10^{-3}$ $m_0 c$. This momentum range represents mainly the annihilations with low-momentum valence electrons. The high-momentum parameter W is the fraction of counts in the wing areas of the peak, with 11×10^{-3} $m_0 c \lesssim p_L \lesssim 29 \times 10^{-3}$ $m_0 c$, arising from annihilations with high-momentum core electrons. The narrowed positron-electron momentum distribution at vacancies is thus experimentally detected as an increase in the S parameter and a decrease in the W parameter. At defects with no open-volume such as in negative ion-type impurities both S and W parameters have the same values as in defect-free lattice.

Depth profiling of the defects in the GaN layers is possible by using a variable energy positron beam. With the positron energy in the range of 0–40 keV it is possible to scan the GaN layers from the surface down to the mean penetration depth of ~2.4 μm. At a given energy E, the S parameter is a linear superposition of values S_i characterizing different positron annihilation states,[20]

$$S(E) = \eta_S(E)S_S + \eta_L(E)S_L + \eta_{\text{Subs}}(E)S_{\text{Subs}}. \qquad (1)$$

In Eq. (1) S_S, S_L, and S_{Subs} are the characteristic S parameter values for positron annihilation at the sample surface, inside the GaN layer, and in the substrate, respectively. The weighting factor η_i is the fraction of positron annihilations at each state. When the GaN layer contains defects which can trap positrons, we can write

$$\eta_L(E)S_L = \eta_b(E)S_b + \sum_i \eta_{d_i}(E)S_{d_i}, \qquad (2)$$

where S_b and S_{d_i} characterize the annihilations in the perfect GaN lattice and in the defect i, respectively. If all positron annihilations take place in the layer ($\eta_L = 1$) containing only a single type of vacancy defects, the concentration of vacancies can be estimated as[20]

$$c_V = \frac{N_{\text{at}}}{\mu_V \tau_b} \frac{(S/S_b - 1)}{(S_V/S_b - S/S_b)}, \qquad (3)$$

where N_{at} is the atomic density, $\tau_b = 165 \pm 1$ ps is the positron lifetime in the GaN lattice,[25] and μ_V the positron trapping coefficient at the vacancy.

C. Secondary ion mass spectrometry

The concentration of oxygen was determined by SIMS analysis using 12 keV cesium primary ions. The primary ion current was 150 nA and analyzed area 350×360 μm^2. The samples were sputter coated with a thin Au layer (thickness 20 nm) in order to avoid sample charging. In addition to this an electron beam (energy 9 keV, current about 1 μA) was used. The SIMS instrument was calibrated for oxygen using ion implanted samples; a known amount of oxygen was implanted to undoped epitaxial GaN layers, where residual oxy-
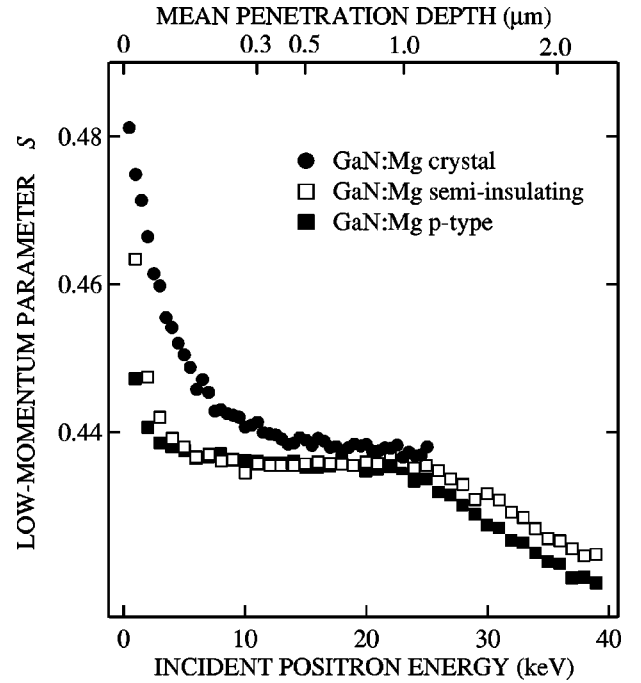

FIG. 1. The low-momentum parameter S as a function of the incident positron energy in p-type and semi-insulating Mg-doped layers and in Mg-doped GaN bulk crystal. The positron mean penetration depth is indicated by the top axis.

gen concentration was well below 10^{18} cm^{-3}. Both oxygen isotopes 16 and 18 were implanted to a dose of 10^{15} cm^{-2}. The depth scale in the depth profiles was determined with a stylus profilometer.

III. RESULTS

A. Mg-doped GaN layers

Figure 1 shows the S parameters measured as a function of incident positron energy at room temperature in SI and p-type GaN:Mg layers and in GaN:Mg single crystal. As the positron energy is increased, the S parameter in the Mg-doped bulk crystal decreases from the surface specific value towards a constant $S \approx 0.435$, which characterizes the bulk properties of the crystal. The thickness of the studied p-type GaN overlayers was about 1 μm. In both epitaxial samples the plateau of the constant $S \approx 0.435$, observed in the energy range 5–25 keV, characterizes the annihilations inside the GaN layer. At higher positron energies part of the positrons annihilate in Al_2O_3 substrate leading to a decrease in S. In fact, the S parameter of $S \approx 0.41$ was determined for Al_2O_3 by implanting positrons into it from the substrate side.

The positron lifetime experiments[25] on the Mg-doped bulk crystal yield a single lifetime component of 165 ps, which corresponds to positron annihilation in delocalized state in the GaN lattice. The Doppler broadening parameters recorded in this sample can thus be used as a reference level characterizing the positron annihilation in a vacancy-free GaN lattice.

The layer-specific parameters both in semi-insulating and in p-type GaN layers are equal to those measured in Mg-
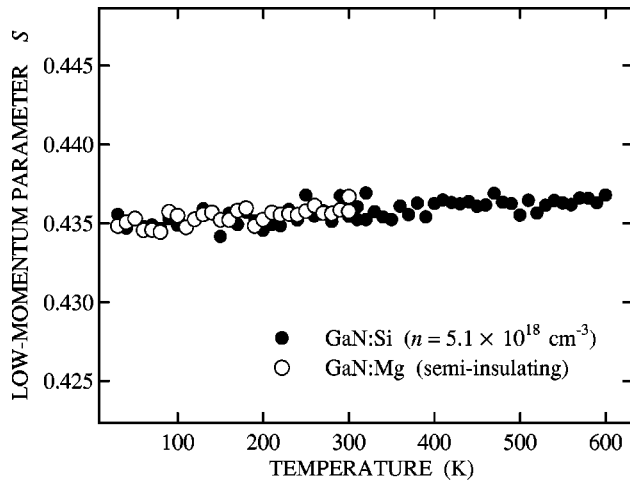
FIG. 2. The low-momentum parameter S as a function of the measurement temperature in semi-insulating layer and in Si-doped layer, measured at incident positron energies of 15 and 30 keV, respectively. The small gradual increase in S with temperature can be attributed to thermal expansion of the lattice.

FIG. 3. The low-momentum parameter S vs. positron incident energy in two undoped GaN layers. The solid lines are guides to the eye.

doped GaN bulk crystal, indicating that in Mg-doped layers the positrons are not trapped at vacancies. Further support to this result was obtained by measuring the layer-specific parameters as a function of temperature. The measurement was done using the positron energy 15 keV, which was chosen to make sure that all annihilations take place inside the GaN layer and not in the substrate nor on the sample surface. Figure 2 shows the temperature behavior of the S parameter in the semi-insulating layer; a similar result is also obtained in the p-type sample. The S parameter in Mg-doped samples increases only a little, $\sim 0.1\%/100$ K, as the temperature is varied between 30–300 K, which is typical for free positron annihilation when the lattice slightly expands with increasing temperature.[20] We thus conclude that positron trapping at vacancy-type defects is not observed in Mg-doped GaN layers. The result, however, does not confirm that the samples are totally free of open-volume defects: vacancies, such as V_N, in positive charge states cannot trap positrons due to the repulsive potential and although they are present they were not detected.

B. Undoped GaN layers

Figure 3 shows the $S(E)$ curves measured in two nominally undoped GaN layers, with the thicknesses of about 0.6 and 1 μm. The reference level corresponding to positron annihilation in a vacancy free lattice is indicated by the curve measured in the p-type layer. A plateau of the S parameter, which characterizes the annihilations in GaN layer, can be found in undoped samples in energy ranges of 7–15 and 7–22 keV. The S parameter in undoped layers is clearly higher than in the p-type reference sample, indicating positron trapping at vacancy-type defects.

The number of different positron traps present in samples can be studied by investigating the linearity between the annihilation parameters S and W.[20] In all studied undoped GaN samples the (S,W) points fall on the same line in the $S-W$
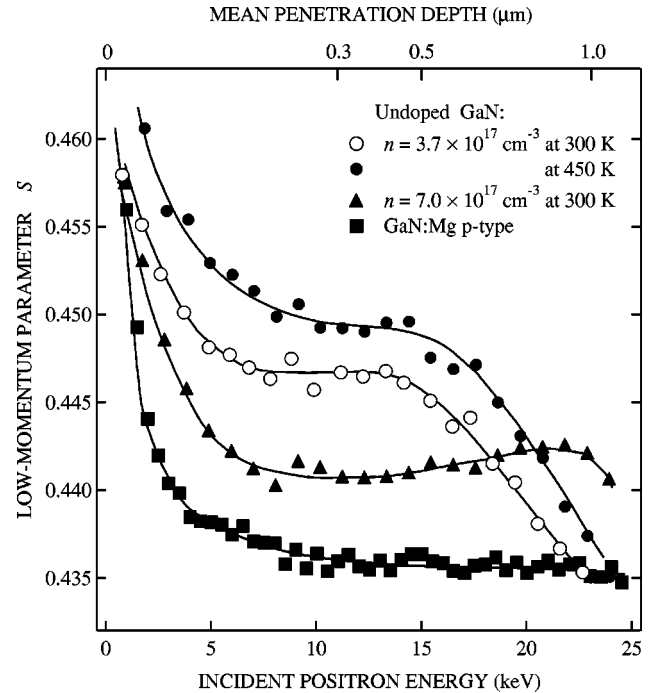
plane as presented in earlier reports[16,24] for both GaN layers and bulk crystals thus showing that the vacancy in all undoped samples is the same. This vacancy has been previously observed in n-type GaN bulk crystals[24,25] where the lifetime of 235 ps has been measured for positrons trapped at the vacancy. Theoretical calculations[27] show that both Ga and N vacancies are able to localize the positron. However, the calculated lifetime at V_{Ga} (209 ps) is much longer than that at V_N (160 ps), reflecting the larger open volume of V_{Ga}. The experimental lifetime of 235 ps is much too long to be due to V_N, but can be well attributed to V_{Ga}. The agreement between calculated and experimental positron lifetime is particularly good[27] if we assume that the neighboring N atoms relax slightly outwards ($\sim 5\%$), as expected from the theory.[14,17] Further support for the identification of V_{Ga} is obtained from the core electron momentum distribution, recorded using the two detector coincidence technique.[23,24]

The combination of positron lifetime and Doppler broadening experiments thus unambiguously shows that the native vacancies in GaN layers belong to the Ga sublattice and have an open volume of a monovacancy. According to theoretical calculations,[14,17] the Ga vacancy is negatively charged in n-type and semi-insulating GaN and thus acts as an efficient positron trap. On the other hand, the N vacancy is expected to be positive and repulsive to positrons.[14] Unfortunately, the present positron experiments do not give direct information if V_{Ga} is an isolated defect or part of a larger complex.

The structural quality of GaN layers on sapphire is dominated by the threading dislocations present at typical concentrations of 10^8–10^{10} cm^{-2}.[28,29] These extended defects originate from the large lattice mismatch between GaN and Al_2O_3. In homoepitaxial growth the density of dislocations
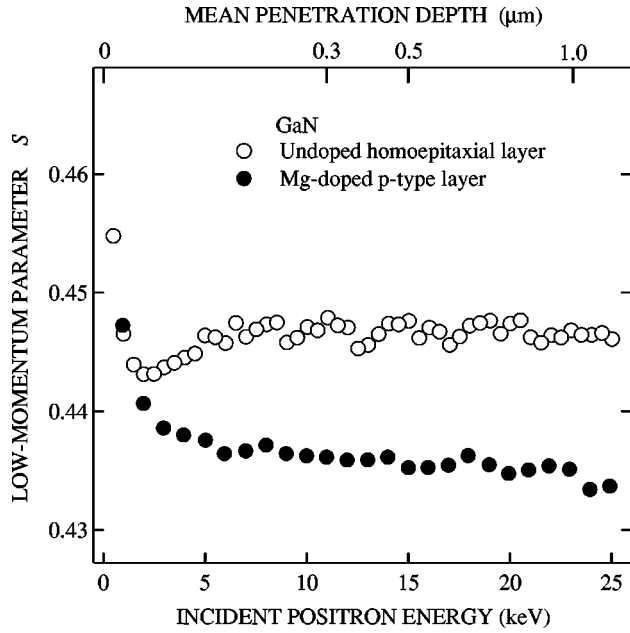
FIG. 4. The S parameter vs. positron incident energy in ho-moepitaxially grown undoped GaN layer. The curve measured in Mg-doped layer is shown as a vacancy-free reference level. The high S parameter indicates vacancy trapping on the epitaxial layer side, but on the substrate side, in the GaN:Mg bulk crystal, the vacancies are not observed.

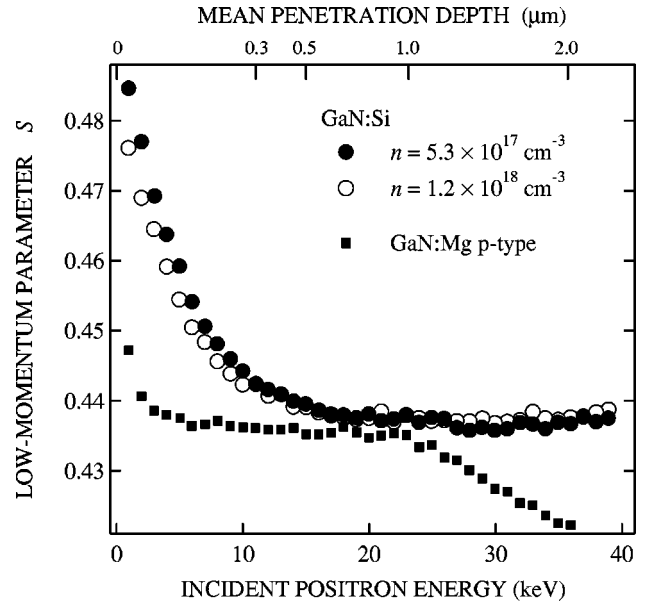FIG. 5. The low-momentum parameter S vs. positron incident energy in two Si-doped GaN layers. The curve measured in p-type GaN layer is shown as a reference level.

$T^{-0.5}$ dependence.[20] The resulting vacancy concentrations, 10^{17}–10^{18} cm^{-3}, are given for each sample in Table I.

C. Si-doped layers

Figure 5 shows $S(E)$ curves measured at 300 K in two Si-doped layers together with the reference level from the p-type layer. In Si-doped GaN layers (Fig. 5)the S parameter decreases as the positron incident energy increases from its surface specific value to its layer specific value. This coincides with the bulk value S_b measured in p-type GaN layers, indicating that no vacancies are observed in Si-doped GaN. The absence of positron trapping at vacancies is also shown by the temperature dependence of the annihilation parameter. The typical temperature behavior of the S parameter in Si-doped layers is shown in Fig. 2. The S parameter increases only slightly, $\sim 0.1\%/100$ K, as the temperature is increased from 30 to 600 K. This small increase can be totally attributed to the thermal expansion of the lattice.[30] The result thus shows that in studied Si-doped layers positron trapping at Ga vacancies is not observed. If they were present in the lattice, the concentration of vacancies would be below the detection limit, $\leq 10^{16}$ cm^{-3}.

D. Correlation between gallium vacancy and oxygen concentrations

The results above show that Ga vacancies are observed in n-type undoped material, but not in samples where n-type conductivity is achieved by Si doping. In order to confirm the role of oxygen impurities in the formation of Ga vacancies, we studied two 2–4 μm thick samples grown in identical conditions by MOCVD on sapphire. The n-type carrier concentrations and electron mobilities of the samples, determined by Hall measurements, are given in Table II. The

is greatly reduced to values which are close to those in GaN bulk crystals ($<10^4$ cm^{-2}). Figure 4 shows the $S(E)$ curve measured in homoepitaxially grown GaN layer together with the curve measured in the p-type GaN:Mg layer. On the substrate side of GaN:Mg bulk crystal the vacancies are not detected. In the undoped overlayer the high S parameter reveals the presence of Ga vacancies, thus suggesting that the removal of dislocations does not reduce the concentration of vacancies. The independence of the Ga vacancy formation from the layer structural quality is also suggested by the comparison between positron experiments in GaN epilayers and in GaN bulk crystals.[24] In both cases the Ga vacancies are observed in noticeable concentrations in undoped material indicating that Ga vacancies are not solely related to extended structural defects.

The S parameter in undoped samples typically shows an increase with temperature between the temperatures 200 and 400 K.[24] This is seen in Fig. 3, where the S parameter values measured in undoped layer with $n=3.7\times10^{17}$ cm^{-3} at 450 K are clearly higher than the values at 300 K. At lower temperatures positrons can also be trapped at shallow traps, e.g., at shallow Rydberg states around negative ions, leading to a decrease in the S parameter (discussed below). In GaN shallow traps are effective still at 300 K. At high temperatures the effect of shallow traps can be neglected and the concentration of Ga vacancies can be estimated using Eq. (3). We use the value $\mu_V \approx 1\times10^{15}$ s^{-1} for the positron trapping coefficient at Ga monovacancies[20] at 450 K and a ratio $S_V/S_b=1.038$ for the vacancy specific S parameter.[24] For the homoepitaxial layer the vacancy concentration is estimated from the data at 300 K and μ_V is scaled according to

TABLE II. The charge carrier concentrations and mobilities in two samples with clearly differing oxygen content. The oxygen concentrations are determined by SIMS analysis and the Ga vacancy concentrations by positron annihilation experiments.

Doping	n (cm^{-3})	μ ($cm^2\,V^{-1}\,s^{-1}$)	$[O]$ (cm^{-3})	$[V_{Ga}]$ (cm^{-3})
Si	8.4×10^{17}	367	$\leqslant 7 \times 10^{17}$	5×10^{16}
O	8.3×10^{17}	95	$> 10^{19}$	2×10^{17}

carrier concentrations of the samples are almost identical, but one of them was doped with silicon and the other was intentionally contaminated with oxygen. Oxygen concentrations in both samples were determined by SIMS analysis, and are also given in Table II. The oxygen concentration is low, $\leqslant 7 \times 10^{17}$ cm^{-3}, in Si-doped sample and more than one order of magnitude higher in the sample doped with oxygen.

The annihilation parameters were measured as a function of positron implantation energy in both samples. The result showed similar behavior as seen in Figs. 1 and 5: At low energies (E<10 keV) the curves were dominated by the positron diffusion to the sample surface and at high energies (E>30 keV) part of the positrons reached the substrate. Figure 6 shows the S and W parameters as a function of measurement temperature in both samples, measured at a positron energy of 20 keV. With this energy all the positrons annihilate inside the GaN layer. At low temperatures the S and W parameters have almost the same value in both samples and they remain almost constant between T = 30 and 250 K. At temperatures T = 250–350 K there is a steep
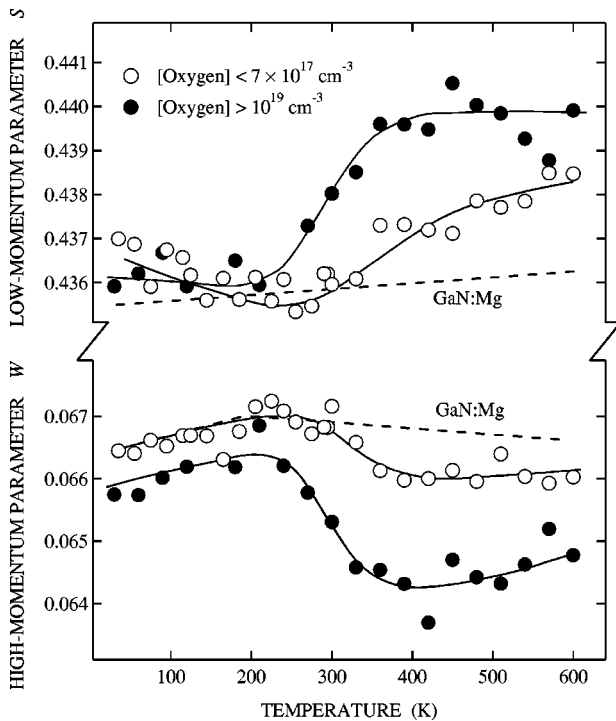

FIG. 6. The line shape parameters S and W as a function of the measurement temperature in two layers with different oxygen content. The solid lines are guides to the eye.

increase in the S parameter, which is followed by an almost constant level at T = 400–600 K.

The constant S parameter level at low temperatures equals the value S_b corresponding to annihilations in lattice with no open volume defects. The increase in the S parameter indicates that positrons are trapped at vacancies as temperature is increased. Positron trapping coefficient at neutral vacancies is independent of temperature and the trapping rate at negative vacancies, such as Ga vacancy, should increase with decreasing temperature.[20] The temperature behavior of the S parameter, as shown in Fig. 6, is typical for positron trapping at two types of defects: At lower temperatures shallow traps, such as negative ion-type defects, compete with vacancy trapping. The annihilation parameters corresponding to positrons trapped at the negative ions are equal to bulk values S_b and W_b, since the defects do not contain any open volume. As the temperature is increased the positrons are able to escape from the shallow traps and the trapping at Ga vacancies is observed. A similar behavior has been previously observed both in undoped GaN epilayers and in GaN bulk samples.[24,25] The Ga vacancy concentrations determined at 500 K using Eq. (3) are shown in Table II.

The higher S and the lower W parameter indicate that Ga vacancies are present in the sample contaminated with oxygen. In the Si-doped sample some V_{Ga} are observed as well, but their concentration is much less than in the O contamined sample. This finding confirms that the presence of oxygen promotes the formation of Ga vacancies in n-type GaN.

IV. FORMATION OF VACANCIES VS. DOPING

Positron experiments detect Ga vacancies in various GaN layers grown by MOCVD on sapphire. The following trends can be summarized for the formation of V_{Ga} as a function of doping: (i) No Ga vacancies are found in p-type or semi-insulating Mg-doped layers. (ii) Ga vacancies are found at concentrations $> 10^{17}$ cm^{-3} in nominally undoped GaN layers, which show n-type conductivity due to residual oxygen. (iii) Much lower Ga vacancy concentrations are observed in samples where the n-type doping is done with Si impurities and the amount of residual oxygen is reduced.

According to the positron experiments the presence of Ga vacancies in GaN layers depends both on the Fermi level and impurity atoms in the samples. The same general trend is found in the epitaxial layers as in the bulk crystals:[25] Ga vacancies are formed only when the Fermi level E_f is close to the conduction band due to n-type doping. For the same position of E_f, n-type doping with oxygen leads to larger concentration of Ga vacancies than Si doping. On the other hand, the presence of oxygen alone does not induce Ga vacancies if the Fermi level is not close to the conduction band. For example, no Ga vacancies are observed in semi-insulating GaN bulk crystals, where the high concentration of O donors is totally compensated electrically by Mg acceptors (E_f at midgap).[25] Furthermore, we detect no Ga vacancies in our Mg-doped GaN layers (samples 1 and 2 in Table I) although the O concentrations of the layers are (2–4) $\times 10^{18}$ cm^{-3} according to SIMS measurements. A natural way to explain all these observations is to infer that Ga va-

cancies and oxygen form complexes, such as V_{Ga}–O_N in *n*-type GaN containing oxygen. In Si-doped GaN the concentration of these complexes is much reduced since O is missing. Smaller concentration of V_{Ga} related defects in some Si-doped samples (Fig. 6) may form due to residual O (leading again to V_{Ga}–O_N formation). It is also possible that other complexes involving V_{Ga}, such as isolated V_{Ga} or V_{Ga}–Si_{Ga} exist in Si-doped GaN.

Theoretically the formation energies of charged defects in thermal equilibrium depend on the position of the Fermi level in the energy gap, as shown by the calculations.[14,17,31] The negatively charged defects such as the Ga vacancy have their lowest formation energy when the Fermi level is close to the conduction band, i.e., in *n*-type material. On the other hand, the formation energy of V_{Ga} is high in semi-insulating and *p*-type material. These trends correlate well with the experimental observations made using positron spectroscopy, where Ga vacancies are observed only in *n*-type material. In fact, the theoretical results predict that the formation energy of V_{Ga}–O_N pair is even lower than that of isolated V_{Ga}.[14] This is consistent with the experimental arguments which associate the observed Ga vacancies mainly with the V_{Ga}–O_N complex. In general, the creation of Ga vacancies (or V_{Ga} complexes) in the growth of both GaN crystals[24,25] and epitaxial layers seems to depend on the Fermi level position as expected for acceptor defects in thermal equilibrium.

The V_{Ga}–O_N complexes may form at the growth temperature when mobile Ga vacancies are trapped by oxygen impurities. Similarly, one could expect the formation of V_{Ga}–Si_{Ga} complexes in Si-doped GaN, as suggested by Kaufmann *et al.*[18] According to the positron experiments, however, the formation of these complexes seems to be less likely than that of V_{Ga}–O_N. According to theory,[17] the binding energy of V_{Ga}–O_N pair (about 1.8 eV) is much larger

than that of V_{Ga}–Si_{Ga} complexes (0.23 eV). The difference in stability is due to the electrostatic attraction: V_{Ga} and O_N are nearest neighbors whereas V_{Ga} and Si_{Ga} are only second nearest neighbors. The V_{Ga}–O_N pairs are thus more likely to survive the cool down from the growth temperature than V_{Ga}–Si_{Ga}. Hence, Ga vacancy complexes are detected by positrons only in materials containing substantial concentrations of oxygen, but their concentration in Si-doped material is much lower. However, the V_{Ga}–Si_{Ga} may be present in some GaN samples (Fig. 6 and Ref. 18) particularly since the formation of Ga vacancies depends also on the stoichiometry of growth conditions.[16]

V. SUMMARY

We have applied positron spectroscopy and secondary ion mass spectrometry to study the influence of doping on the formation of Ga vacancies in heteroepitaxial and homoepitaxial GaN layers. In *p*-type and in semi-insulating Mg-doped layers the Ga vacancies are not observed. Ga vacancies exist in high concentrations in undoped *n*-type GaN layers, where the *n*-type conductivity is due to residual oxygen impurities. Gallium vacancies are found both in layers grown on sapphire and in homoepitaxially grown material where the dislocation density is greatly reduced. This suggests that the formation of Ga vacancies is promoted by the *n*-type doping and does not require the presence of dislocations. In samples where the *n*-type conductivity is achieved by silicon doping, however, clearly less gallium vacancies are observed than in samples containing oxygen. We propose that the presence of oxygen leads to the formation of stable gallium vacancies complexed with oxygen impurities. This conclusion is in good agreement with theoretical calculations predicting low formation energy and high binding energy for V_{Ga}–O_N complex in *n*-type GaN.

[1] F. A. Ponce, D. Cherns, W. T. Young, and J. W. Steeds, Appl. Phys. Lett. **69**, 770 (1996).

[2] Z. Liliental-Weber, Y. Chen, S. Ruminov, and J. Washburn, Phys. Rev. Lett. **79**, 2835 (1997).

[3] J. Elsner, R. Jones, P. K. Sitch, V. D. Porezag, M. Elstner, Th. Frauenheim, M. I. Heggie, S. berg, and P. R. Briddon, Phys. Rev. Lett. **79**, 3672 (1997).

[4] A. F. Wright and U. Grossner, Appl. Phys. Lett. **73**, 2751 (1998).

[5] J. S. Speck and S. J. Rosner, Physica B **273–274**, 24 (1999).

[6] D. C. Look and J. R. Sizelove, Phys. Rev. Lett. **82**, 1237 (1999).

[7] J. Neugebauer and C. G. Van de Walle, Phys. Rev. B **50**, 8067 (1994).

[8] D. C. Look, D. C. Reynolds, J. W. Hemsky, J. R. Sizelove, R. L. Jones, and R. J. Molnar, Phys. Rev. Lett. **79**, 2273 (1997).

[9] J. Neugebauer and C.G. Van de Walle, in *Gallium Nitride and Related Materials*, edited by F.A. Ponce, R.D. Dupuis, S. Nakamura, and J.A. Edmond, MRS Symposia Proceedings No. 395 (Materials Research Society, Pittsburg, 1996), p. 645.

[10] T. L. Tansley and R. J. Egan, Phys. Rev. B **45**, 10 942 (1992).

[11] P. Perlin, T. Suski, H. Teisseyre, M. Leszczynski, I. Grzegory, J. Jun, S. Porowski, P. Boguslawski, J. Bernholc, J. C. Chervin, A. Polian, and T. D. Moustakas, Phys. Rev. Lett. **75**, 296 (1995).

[12] W. Götz, N. M. Johnson, C. Chen, H. Liu, C. Kuo, and W. Imler, Appl. Phys. Lett. **68**, 3144 (1996).

[13] C. Wetzel, T. Suski, J. W. AgerIII, E. R. Weber, E. E. Haller, S. Fischer, B. K. Meyer, R. J. Molnar, and P. Perlin, Phys. Rev. Lett. **78**, 3923 (1997).

[14] T. Mattila and R. M. Nieminen, Phys. Rev. B **55**, 9571 (1997).

[15] G.-C. Yi and B. W. Wessels, Appl. Phys. Lett. **69**, 3028 (1996).

[16] K. Saarinen, P. Seppälä, J. Oila, P. Hautojärvi, C. Corbel, O. Briot, and R. L. Aulombard, Appl. Phys. Lett. **73**, 3253 (1998).

[17] J. Neugebauer and C. G. Van de Walle, Appl. Phys. Lett. **69**, 503 (1996).

[18] U. Kaufmann, M. Kunzer, O. Obloh, M. Maier, Ch. Manz, A. Ramakrishnan, and B. Santic, Phys. Rev. B **59**, 5561 (1999).

[19] P. J. Schultz and K. G. Lynn, Rev. Mod. Phys. **60**, 701 (1988).

[20] K. Saarinen, P. Hautojärvi, and C. Corbel, in *Identification of Defects in Semiconductors*, edited by M. Stavola (Academic Press, New York, 1998), p. 209.

[21] R. Krause-Rehberg and H.S. Leipner, *Positron Annihilation in*

Semiconductors (Springer-Verlag, Berlin, 1999).

[22] M. J. Puska and R. M. Nieminen, Rev. Mod. Phys. **66**, 841 (1994).

[23] L. V. Jorgensen, A. C. Kruseman, H. Schut, A. Van Veen, M. Fanciulli, and T. D. Moustakas, in *III-V Nitrides*, edited by F. A. Ponce, T. D. Moustakas, I. Akasaki, and B. A. Monemar, MRS Symposia Proceedings No. 449 (Materials Research Society, Pittsburg, 1997), p. 853.

[24] K. Saarinen, T. Laine, S. Kuisma, J. Nissilä, P. Hautojärvi, L. Dobrzynski, J. M. Baranowski, K. Pakula, R. Stepniewski, M. Wojdak, A. Wysmolek, T. Suski, M. Leszczynski, I. Grzegory, and S. Porowski, Phys. Rev. Lett. **79**, 3030 (1997).

[25] K. Saarinen, J. Nissilä, P. Hautojärvi, J. Likonen, T. Suski, I. Grzegory, B. Lucznik, and S. Porowski, Appl. Phys. Lett. **75**, 2441 (1999).

[26] A. M. Witowski, M. L. Sadowski, K. Pakula, B. Suchanec, R. Stepniewski, J. M. Baranowski, M. Potemski, G. Martinez, and P. Wyder, MRS Internet J. Nitride Semicond. Res. **3**, 33 (1998).

[27] K. Saarinen, J. Nissilä, J. Oila, V. Ranki, M. Hakala, M. J. Puska, P. Hautojärvi, J. Likonen, T. Suski, I. Grzegory, B. Lucznic, and S. Porowski, Physica B **273–274**, 33 (1999).

[28] S. D. Lester, F. A. Ponce, M. G. Craford, and D. A. Steigerwald, Appl. Phys. Lett. **66**, 1249 (1995).

[29] X. H. Wu, L. M. Brown, D. Kapolnek, S. Keller, B. Keller, S. P. DenBaars, and J. S. Speck, J. Appl. Phys. **80**, 3228 (1996).

[30] S. Kuisma, K. Saarinen, P. Hautojärvi, C. Corbel, and C. LeBerre, Phys. Rev. B **53**, 9814 (1996).

[31] P. Boguslawski, E. L. Briggs, and J. Bernholc, Phys. Rev. B **51**, 17 255 (1995).